Journal of Applied Polymer Science

α-Thiophene end-capped styrene copolymer containing fullerene pendant moieties: Synthesis, characterization, and gas sensing properties

Erdem Şennik,[1,2] Büşra Şennik,[3,4] Onur Alev,[1] Necmettin Kılınç,[2,5] Faruk Yilmaz,[3] Zafer Ziya Öztürk[1]

[1]Department of Physics, Gebze Technical University, Kocaeli 41400, Turkey
[2]Nanotechnology Application and Research Center, Nigde University, Nigde 51245, Turkey
[3]Department of Chemistry, Gebze Technical University, Kocaeli 41400, Turkey
[4]Department of Chemistry, Istanbul Medeniyet University, Istanbul 34720, Turkey
[5]Department of Mechatronics Engineering, Nigde University, Nigde 51245, Turkey
Correspondence to: E. Şennik (E-mail: erdemsennik@gmail.com or esennik@gtu.edu.tr) and F. Yilmaz (E-mail: fyilmaz@gyte.edu.tr)

ABSTRACT: We report the synthesis, characterization, and gas sensing properties of a styrene copolymer bearing α-thiophene end group and fullerene (C_{60}) pendant moieties P(S-*co*-CMS-C_{60}). First, the copolymer of styrene (S) and chloromethylstyrene (CMS) monomers was prepared in bulk via a bimolecular nitroxide-mediated radical polymerization (NMP) technique using benzoyl peroxide (BPO) as the radical initiator and nitroxy-functional thiophene compound (Thi-TEMPO) as the co-radical and this gave α-thiophene end-capped copolymer P(S-*co*-CMS). The chloromethylstyrene units of P(S-*co*-CMS) allowed further side-chain functionalization onto P(S-*co*-CMS). The obtained P(S-*co*-CMS) was then reacted with sodium azide (NaN_3) and this led to the copolymer with pendant azide groups, P(S-*co*-CMS-N_3), and then grafted with electron-acceptor C_{60} via the reaction between N_3 and C_{60}. The final product was characterized by using NMR, FTIR, and UV–vis methods. Electrical characterization of P(S-*co*-CMS-C_{60}) thin film was also investigated at between 30 and 100 °C as the ramps of 10 °C. Temperature dependent electrical characterization results showed that P(S-*co*-CMS-C_{60}) thin film behaves like a semiconductor. Furthermore, P(S-*co*-CMS-C_{60}) was employed as the sensing layer to investigate triethylamine (TEA), hydrogen (H_2), acetone, and ethanol sensing properties at 100 °C. The results revealed that P(S-*co*-CMS-C_{60}) thin film has a sensing ability to H_2. © 2016 Wiley Periodicals, Inc. J. Appl. Polym. Sci. **2016**, *133*, 43641.

KEYWORDS: band structure; electrical characterization; fullerene; gas sensor; polystyrene; thin film

Received 25 November 2015; accepted 10 March 2016
DOI: 10.1002/app.43641

INTRODUCTION

There has been growing interest in polymers because of their wide range of potential applications such as coating, adhesive, packaging, clothing, engineering, structural material, electronic, and medical to name a few.[1–7] A key feature of the versatility for these materials is that it is possible to incorporate various organic molecules into polymers with different topologies such as linear, cyclic, star, branched, and dendritic.[8]

A particular feature of polymers is possibility of obtaining well-defined structure by controlled radical polymerization (CRP) techniques which carry tailored functional groups and have been shown to be critical for a range of potential applications.[9] There has been significant attention from both academic and industrial communities for CRP techniques due to its versatility in the synthesis of polymers with predictable molecular weights, low dispersities and specific functionalities, and its general applicability for a wide range of monomers.[10]

Polymers can be functionalized at both side chain[11] and chain end[12] to improve their properties for different applications. Fullerene (C_{60}) is one of the most popular examples to be functionalized.[13,14] There is a massive drive to understand C_{60} (Fullerene) derivatives and improve their properties in last decade since C_{60}'s interesting properties such as conducting,[15] gas sensing,[16] photovoltaic,[17] and electrical[18] have been observed. However, many of its potential applications have been limited by its poor solubility and processability.[19] To overcome this problem, polymers have been functionalized with C_{60}. Incorporating of C_{60} into polymer chain is a practical way to improve its solubility.[20]

C_{60} containing polymers can be prepared by incorporating C_{60} into the backbone of polymer chains or by attaching C_{60} onto

tailor-made functional polymers.[21] The attachment of the C_{60} group onto polymer chains brings attractive properties. For instance, C_{60}-functionalized conjugated polyesters have been used as photovoltaic cells and electroluminescent devices. Nava *et al.* reported that fullerene-containing polyesters are easy to process, thus making them interesting candidates for materials science applications due to their good solubility in common organic solvents and good film-forming properties.[22] Electroluminescent (EL) properties of C_{60}-containing polymer were investigated by Lee *et al.* They found that quantum efficiency and the emitted light power were improved by ≈5 and ≈20 times. These features of C_{60}-containing polymer give hope for its application in many different fields of optoelectronics.[23] Furthermore, as expected, several polymers showed outstanding properties such as optical limiting[24] and photoinduced electron transfer.[25]

H_2 and TEA are flammable and hazardous gases whose detection is an important issue. To sense these gases, metal oxides are generally utilized as a sensing layer but in recent years conducting polymers are widely being used. Conducting polymer composites with other polymers such as Nylon 6, poly(vinyl alcohol) (PVA), and poly (methyl metharylate) (PMMA) are also used to detect such gases.[26,27] Polystyrene (PS) is a remarkable material that has been used in several areas from building to sensor in recent years.[28] It has been chosen as a sensing material to detect risky gases with some carbon compounds in composite form. For instance Li *et al.* focused on response of carbon black filled PS composites against various organic vapor environments and found that composites would be good candidate for practical application.[29] PS was also selected as the matrix polymer while multiwalled carbon nanotubes (MWCNTs) were used as fillers. The composites synthesized through polymerization-filling exhibit significant responsivity to the organic vapors.[30]

To investigate gas sensing properties, there are many papers about polymer composites with carbon compounds, but there is no study about C_{60}-based polymer gas sensors. In this work, we report the preparation of α-thiophene end capped styrene copolymer bearing C_{60} side groups P(S-*co*-CMS-C_{60}) with the motivation of investigating the effect of pendant C_{60} groups on the gas sensing behaviors for triethylamine (TEA) and hydrogen (H_2). In this field about C_{60}'s sensing properties towards H_2, there is only one paper reported by Sberveglieri *et al.*, where the sensor was fabricated in harsh condition using vacuum sublimation of C_{60}. They also observed a reversible increase of the current in the presence of hydrogen at 300 °C.[31] On the other hand, in this study, the sensor was obtained via spin coating method by employing C_{60} containing styrene based soluble copolymer. The fabricated sensor has also a better sensitivity even at 100 °C. The modified polymers were characterized using Fourier transform infrared (FTIR), ^{1}H-NMR, UV–vis spectroscopy, and gel permeation chromatography (GPC), as well as differential scanning calorimetry (DSC) and thermogravimetric analysis (TGA). In addition, the electronic properties and gas sensing characteristics of P(S-*co*-CMS-C_{60}) thin film were investigated at desired temperature. The results revealed that the thin film has a feature of an electronically semiconductor and also a good sensor property toward H_2.

EXPERIMENTAL

Materials and Instruments

Styrene (S, 99%, Fluka,) was passed through a column of basic alumina to remove inhibitor before use. Chloromethylstyrene (CMS, 90%, Aldrich,) was distilled under vacuum immediately before use. Benzoyl peroxide (BPO) was recrystallized from methanol/chloroform (1:1) mixture. Methanol (99.9%, Merck) was dried over activated 4-Å molecular sieves and distilled before using. Dichloromethane (DCM, 99.8%, Merck,) was dried over phosphorus pentoxide. *N,N*-Dimethylformamide (DMF, 99.8%, Merck) was both dried and stored over activated 4-Å sieves. Tetrahydrofuran (THF, 99.8%, Merck) was dried by refluxing over Na-K alloy and then distilled in a dry argon atmosphere. Fullerene (C_{60}, 98%, Aldrich), sodium azide (NaN_3, 99.5%, Sigma Aldrich), magnesium sulfate (98%, Merck), sodium sulfate (99%, Merck), 1,2-dicholorobenzene (DCB, 99%, Merck), chloroform (99%, Merck) were used as purchased without further purification. Nitroxy-functional thiophene compound (Th-TEMPO) was synthesized according to the reported procedure.[32]

^{1}H-NMR and ^{13}C-NMR spectra were recorded in $CDCl_3$ solution on a Varian UNITY INOVA 500 MHz spectrometer. FTIR spectra were recorded on Perkin–Elmer Paragon 1000 spectrometer. UV–vis was recorded using 1-cm path length cuvettes on Shimadzu 2001UV. Average molecular weights and molecular weight distributions of the polymers were determined on an Agilent GPC Instrument (Model 1100) consisting of a pump, a refractive index detector and two Waters Styragel columns (HR, 5E and HR 4E) and using THF as eluent at a flow rate of 0.5 mL min^{-1} at 23 °C. Thermogravimetric analysis (TGA) was performed on a Mettler Toledo TGA/SDTA 851 thermogravimetric analyzer with a heating rate of 10 °C min^{-1} from room temperature to 700 °C under nitrogen atmosphere. Glass transition temperatures (T_g) of the polymers were determined on a Pelkin Elmer DSC 8500 under nitrogen flow (20 mL min^{-1}). The copolymers were first heated from 0 to 200 °C at a heating rate of 10 °C min^{-1} and then they were cooled to 0 °C at 10 °C min^{-1} to erase the thermal history. Finally they were heated again to 200 °C at 10 °C min^{-1}. Electrochemical measurements were performed with a Potentiostat (CHI70514) using a Pt working electrode, an Ag/Ag$^+$ reference electrode ($AgNO_3$ (10 mM) in 0.1 *M* Bu_4NBF_4-MeCN) and a Pt counter electrode. Bu_4NBF_4 was used as supporting electrolyte in 1,2-dichlorobenzene, concentration of analyte 1 mM and the scan rate was 20 mV s^{-1}.

Spin coater was used for coating P(S-*co*-CMS-C_{60}) on a glass slide. Gold (Au) interdigital electrodes (IDEs) were evaporated onto the samples with a thermal evaporation system (Leybold Univex 450). The dc measurements were performed with an electrometer (Keithley 6517A). Gas flow meters were controlled with multi gas controller device (MKS 647C). Temperature controller device (Lakeshore 340) was used to keep the desired temperature of sensors.

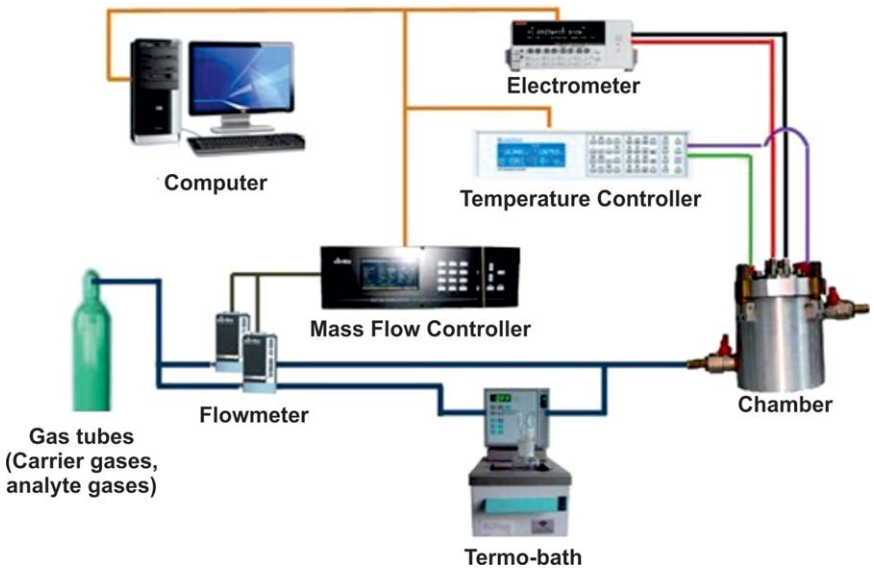

Figure 1. Electrical and gas measurement system. [Color figure can be viewed in the online issue, which is available at wileyonlinelibrary.com.]

Synthesis of P(S-*co*-CMS), P(S-*co*-CMS-N_3), and P(S-*co*-CMS-C_{60})

Side chain chlorine and azide containing polymers P(S-*co*-CMS) (P1) and P(S-*co*-CMS-N3) (P2) were synthesized according to our previous work.[33] P(S-*co*-CMS-C_{60}) (P3) was prepared as follows: A mixture of P(S-*co*-CMS-N_3) (P2) (0.7 g, 0.063 mmol), C_{60} (0.055 g, 0.076 mmol) and 150 mL 1,2-dichlorobenzene was placed in a round bottom flask and degassed by bubbling argon for 10 min. The homogeneous reaction mixture was stirred at 60 °C under argon for 2 days. The solution was heated 130 °C and allowed to continue overnight again. The resulting mixture was evaporated to dryness and then 30 mL THF was added the residue. The mixture was stirred for 12 h at room temperature. Unreacted C_{60} and other insoluble matters were filtered off. The clean filtrate was evaporated and dried in vacuum desiccator at 25 °C to obtain brown product.

Yield: 0.48 g (64%). $M_{n\text{GPC}}$: 27,000 Da. FTIR (cm^{-1}): 3020 (aromatic CH, Thi, and phenyl rings); 2923–2848 (aliphatic CH); 850 (CH of the Thi ring); 779 (CH of the Thi ring). ^{1}H-NMR ($CDCl_3$, δ, ppm): 7.21, 6.55, and 6.20 (Ar CH in the repeating units); 4.15 (C_6H_4-CH_2-N_3) and 5.0 (C_6H_4-CH_2-C_{60}); 2.0–1.1 (CH and CH_2 in the polymer backbone).

Electrical and Gas Sensing Measurements

For electrical and gas sensing measurements, P(S-*co*-CMS-C_{60}) was coated on a glass slide by using spin coater. Glass substrates were cleaned in acetone, ethyl alcohol, and deionized water using ultrasonic cleaner for each 10 min. P(S-*co*-CMS-C_{60}) solution (10mg/mL in chloroform) was coated on glass substrate at spin rate of 1000 rpm for 60 s.

Current–voltage (*I*–*V*) measurements were performed to investigate the electrical properties of styrene copolymer thin films. For electrical measurements, gold (Au) interdigital electrodes (IDEs) were evaporated onto the samples with a Leybold Univex 450 coater system using a shadow mask. The IDEs consisted of 10 interdigital pairs of Au fingers were deposited on the thin films, with a thickness of 150 nm, a width of 100 μm, and a spacing of 100 μm between adjacent fingers. DC electrical measurements were carried out under a high-purity dry air flow (flow rate: 200 mL/min) in the temperature range of 30–100 °C. The current–voltage (*I*–*V*) measurements were performed with a Keithley 6517A electrometer/high resistance meter in the dark at a sweep rate of 50 mV/s between −1 and 1 V. The data of IV characteristic were plotted with gold (Au) as the metal contact.

Gas-sensing measurements for P(S-*co*-CMS-C_{60}) thin films were performed in a homemade test chamber (1 L) connected to a high-purity dry air line. The experimental procedure was performed by heating the devices up to 100 °C under the high purity dry air (200 sccm) flow. After that, the admirable concentrations of the gas were sent into the gas chamber. While H_2 gas was directly sent into the chamber from the gas tube, TEA was different. TEA (50 mL) was placed in a glass washing bottle that was put inside thermostatic bath maintained at a certain temperature to provide the appropriate partial pressure. We used gas flow meters controlled with multi gas controller device (MKS 647C) were used to adjust desired concentration of TEA gas. A schematic figure of gas test system is given in Figure 1. Temperature controller device (Lakeshore 340) was used to keep the desired temperature of sensors. The gas test chamber (1L) reached the maximum gas concentration with flow of 200 sccm for 5 min. The bias voltage of 1 V was applied to the sensor. The direct current (dc) was measured with a Keithley 6517A Electrometer/High Resistance Meter. The dc (sensitivity) was monitored continuously under dry air flow and recorded using an IEEE 488 data acquisition system incorporated into a personal computer. The high purity dry air flowed through the test chamber for almost 15 min, and then exposed TEA at 5000 ppm through a bubbler.

RESULTS AND DISCUSSION

Structural and optical characterization

P(S-*co*-CMS-C_{60}) was synthesized in three step reaction-sequence. First step was nitroxide mediated copolymerization of

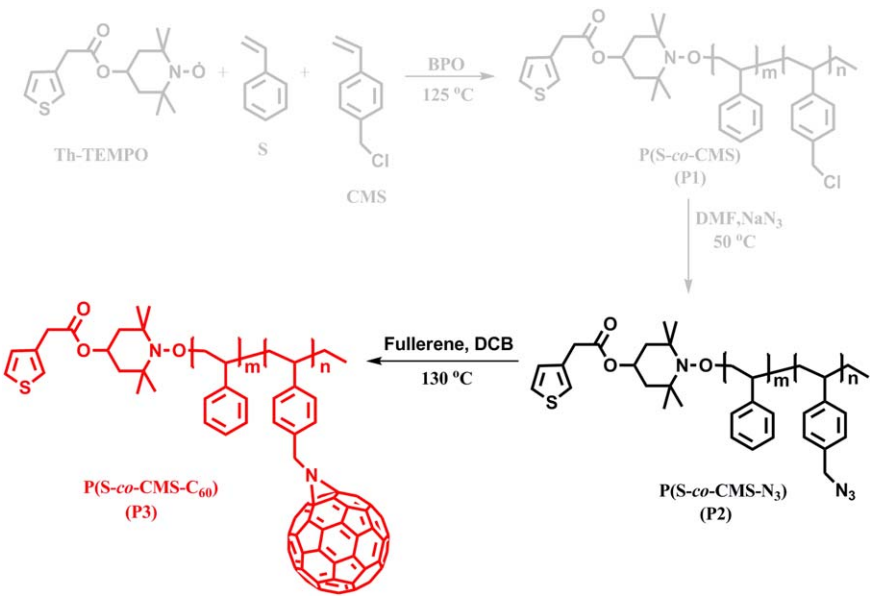

Figure 2. The synthesis of thiophene end-capped polystyrene with fullerene side chain. [Color figure can be viewed in the online issue, which is available at wileyonlinelibrary.com.]

monomers and the other steps were post-functionalization of the copolymer to obtain the side chain fullerene functional copolymer. It was demonstrated that nitroxide mediated polymerization (NMP) is a suitable technique for synthesizing the well-defined monosubstituted C_{60}-containing polymer. The synthetic routes of the copolymers are depicted in Figure 2. To avoid multiple substitutions of P(S-*co*-CMS-N_3) chains onto the same C_{60} and the formation of C_{60} charge transfer complex, a higher ratio of C_{60}/P(S-*co*-CMS-C_{60}) (1.2:1) was used.[34] The molecular structures of the copolymers were verified by FTIR and ^{1}H-NMR. The data related to molecular weights and polydispersities of the synthesized polymers were obtained by GPC. The thermal properties of the copolymers were investigated by TGA and DSC.

^{1}H-NMR spectra of P2 and P3 are shown in Figure 3(a,b). ^{1}H-NMR spectrum of P1 shows chemical shifts at $\delta = 4.00$-4.15 ppm for –C$\boldsymbol{H_2}$N$_3$ groups, $\delta = 1.1$–2 ppm for –C$\boldsymbol{H_2}$ and –C$\boldsymbol{H}$ groups in the polymer backbone, $\delta = 6.20$-7.20 ppm for aromatic protons of phenyl groups. The copolymer composition was determined by ^{1}H-NMR by comparing the integral peak areas of the protons at 4.00-4.15 ppm and those at 6.20-7.20 ppm, which is in good agreement with the feed ratio of the monomers. The resonance peaks of the H_a methylene protons next to the phenyl ring in the CMS repeating units moved upfield from 4.40 ppm to 4.00–4.15 ppm in the ^{1}H-NMR spectrum of P2 [Figure 3(a)] as a result of azidification.[33] Upon grafting of C_{60}, the signals of H_a methylene protons connected to C_{60} shifted downfield to 4.93 and H_a methylene protons connected to N_3 still exist at 4.13 ppm in the ^{1}H-NMR spectrum of P3 in Figure 3(b). These NMR results showed that 65% of azide group was converted to C_{60}. The successful covalent atthacment of C_{60} to P2 as the side group was further supported by the evidence from ^{13}C-NMR as shown in Figure 3(c). In the ^{13}C-NMR spectrum of P3, the signal of the carbon atoms of C_{60} units was observed at $\delta = 135$ ppm, clearly indicating the incorporation of C_{60}.

FTIR spectra at Figure 4 showed absorption of aromatic C-C band at 2900 cm^{-1}. After azidification reaction, FTIR spectra showed a new absorption at 2075 cm^{-1} for –N_3 groups. This result explicitly confirmed that the chloride functional groups were converted into azide functional groups. The progress of linking of fullerene to the copolymer as aside group was monitored by infrared spectroscopy. After refluxing for two days, the color of the reaction solution turned into brown and although ^{1}H-NMR results show partially conversion of N_3 to C_{60} the strong band of azide groups at 2075 cm^{-1}in FTIR spectrum completely disappeared.[35]

The number-average molecular weights of the copolymers along with their PDI (polydisperity index) values were measured by GPC and related data are summarized in Table I. All the copolymers showed unimodal elution peaks. The molecular weight of the C_{60} containing copolymer is higher than those of the precursor copolymers, indicating that C_{60} has been incorporated into the polymer chain.[36]

The glass transition temperatures of the polymers were investigated by DSC analysis. The related T_g results are shown in Table II. The T_g value of copolymer increased as incorporation of pendant C_{60} moiety imparts rigidity and restricts the movements of the polymer chains.[37] Katiyar *et al.* synthesized C_{60} containing PMMA and reported that T_g increases with the increase of fullerene content in the polymers.[38] The decomposition thermograms of the copolymers and pristine C_{60} were carried out under N_2 atmosphere with a heating rate of 10 °C/min. The TGA thermograms and the related data are presented in Figure 5 and Table II, respectively. Both P2 and P3 exhibited a distinct decomposition step which occurred at around 360 °C and it is attributed to the loss of copolymer backbone.

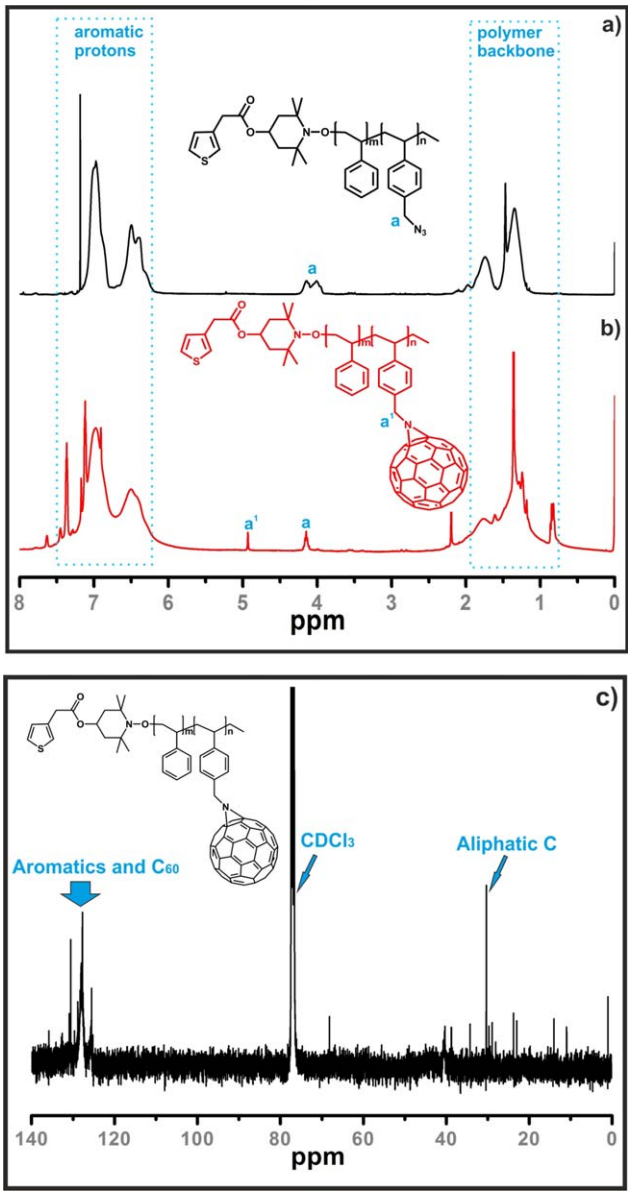

Figure 3. ^{1}H-NMR spectra of (a) P2, (b) P3, and (c) ^{13}C-NMR spectrum of P3 in $CDCl_3$ at ambient temperature. [Color figure can be viewed in the online issue, which is available at wileyonlinelibrary.com.]

Compared to char yield of P2 and P3, the incorporation of C_{60} as the side group improved the thermal stability of the copolymer. As C_{60} is thermally stable up to 600 °C, the % weight of C_{60} in P3 can be calculated by subtracting the residue mass of P2 from the mass remained at the end point of analysis at 650 °C. The procedure is based on the assumption that other than C_{60} and N_3 side groups, the residue masses of P2 and P3 should be the same as they have identical chemical compositions. The % weight of C_{60} thus obtained was 15.33, agreeing reasonably well with the calculated from the NMR spectrum.[39]

The electrochemical properties of C_{60} and P3 were investigated by cyclic voltammetry in 1,2-dichlorobenzene as a further proof for attachment of C_{60} to the polymer as a side group . It is well known that C_{60} has multiple and reversible redox behavior.[40,41]

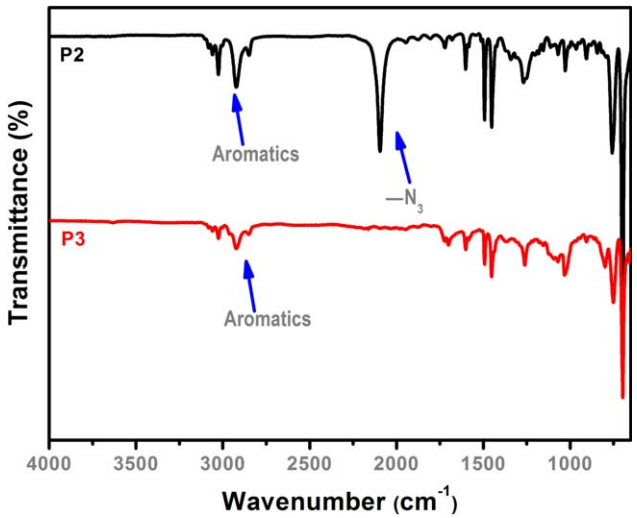

Figure 4. FTIR spectra of P2 and P3. [Color figure can be viewed in the online issue, which is available at wileyonlinelibrary.com.]

As seen in Figure 6 in potential range between 1 V and −3,5 V C_{60} has shown triple reversible peaks on the contrary P3 has shown triple irreversible peaks. It can be seen that the functionalization of C_{60} with polymer makes the oxidation of C_{60} more difficult and irreversible. This can be explained in terms of a stepwise loss of conjugation due to functionalization with polymer. Damlin *et al.* reported similar CV results that the reductions became irreversible with increasing degrees of functionalization of the fullerene cage.[42]

The optical properties of P3 are given in Figure 7. The incorporation of C_{60} as the side group into P3 was also confirmed by the UV–vis spectra as seen in Figure 7(a). P3 is soluble in common organic solvents such as chloroform, toluene, and THF and its solution, which is brown in color, together with P2 is shown in inlet box of Figure 7(a). The covalent attachment of C_{60} onto P2 greatly increased C_{60}'s solubility in organic solvents.[43] As it is clearly seen in the UV–vis spectra, the characteristic peak of C_{60} at 334 nm was also observed in P3, indicating that C_{60} has been successfully grafted to P3. In Figure 7(b), cutoff wavelength (λ_c) value was calculated 419 nm from

Table I. The Results of Thiophene End-Capped Styrene Copolymers with Different Side Functionalities

Polymers	$M_{n,GPC}$[a]	M_w/M_n[a]	Side groups
P1[b]	9400	1.4	-Cl
P2[c]	11,000	1.6	$-N_3$
P3	27,000	2.1	$-C_{60}$

[a] $M_{n,GPC}$ and M_w/M_n were determined by GPC analysis with polystrene standards and THF was used as the eluent (RI detector).
[b] Polymerization conditions: $T = 125$ °C; bulk; polymerization time = 18 h.; [BPO]/[Th-TEMPO] = 1; [S]/[CMS] = 5 in feed and 4.3 in copolymer composition. The composition was calculated by comparing the integral peak areas of the methylene protons next to the benzene ring in CMS at 4.51–4.38 ppm to that of the aromatic benzene protons in CMS and S (7.06–6.49 ppm) (The contribution of the end-group phenyl protons in this range was neglected).[32]

Table II. Thermal Properties of Copolymers

Polymers	T_{onset} (°C)[a]	T_{max} (°C)[b]	Char yield (%)[c]	T_g (°C)[d]
P2	360	404	5.17	93
P3	376	415	20.5	98

[a] T_{onset} is the onset decomposition temperature.
[b] T_{max} is the temperature corresponding to the maximum rate of weight loss.
[c] The percent of char yield at 700 °C.
[d] T_g is the glass transition temperature of the polymers in the second run of DSC experiment.

the intersection of linear line at UV–vis spectrum with *x*-axis. Besides, λ_c value was found to be 420 nm from the equation of linear region (420 nm) in the inlet UV–vis spectrum of Figure 7(b). The UV–vis absorption data of P3 were fitted for both indirect and direct band gap transitions to determine the type of band to band transition. Figure 7(c,d) shows $(\alpha h\nu)^2$ versus $(h\nu)$ for direct transition and $(\alpha h\nu)^{1/2}$ versus $(h\nu)$ for indirect transition, respectively. The straight lines of the curves to the energy axis $(h\nu)$ in Figure 7(c,d) give the band gaps of P3 for direct and indirect transitions. The direct and the indirect band gaps of P3 were found to be 3.28 and 3 eV, respectively. The plots of $(\alpha h\nu)^2$ and $(\alpha h\nu)^{1/2}$ versus $(h\nu)$ in the absorption edge region are shown in the inset of Figure 7(c,d), respectively. If the linearity factors of the plots are calculated for direct and indirect optical transitions, the linearity factors in indirect transition case for the absorption edge of P3 seem to be better. Therefore, the band-to-band transition of P3 could be indirect one and its band gap should be 3 eV. The band gap of P3 (2.96 eV) was also proved to be indirect with eq. (1). It's good agreement that the results of Figure 7(d) and eq. (1) are almost the same. Hence, the band to band transition of P3 might be indirect transition.

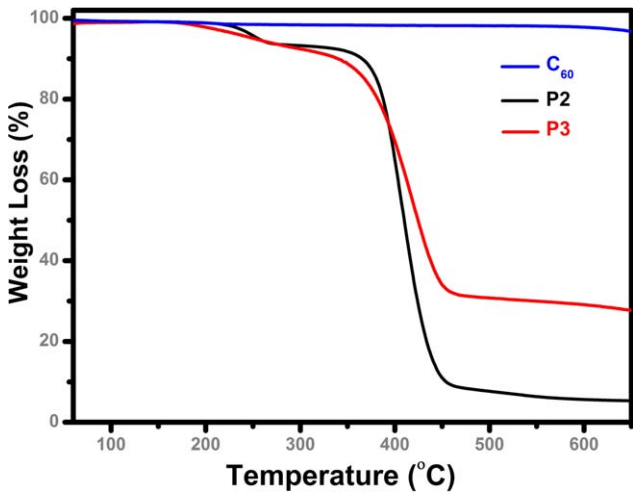

Figure 5. TGA thermograms of pristine C_{60}, P2, and P3. [Color figure can be viewed in the online issue, which is available at wileyonlinelibrary.com.]

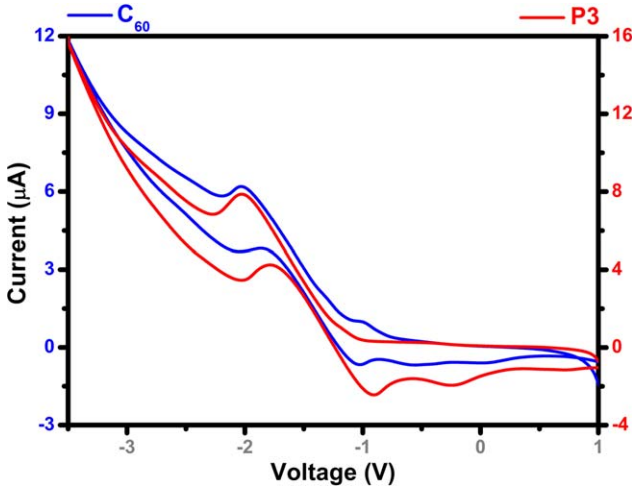

Figure 6. CV for C_{60} and P3 obtained at Pt electrode in the 1,2-dichlorobenzene containing 0.1 *M* $TBABF_4$. Scan rate 20 mV s^{-1}. [Color figure can be viewed in the online issue, which is available at wileyonlinelibrary.com.]

$$E_g = \frac{hc}{\lambda_c} \quad (1)$$

Electrical Characterization

The dc electrical measurements of P3 thin film were performed under high purity dry air flow at the temperature range from 303 to 373 K as seen in Figure 8(a). The closer view of *I–V* measurements at 303 and 323 K is given in Figure 8(b). The *I–V* characteristics of P3 thin film have a hysteresis at all temperatures and the hysteresis increased with increasing temperature. There are several mechanisms for *I–V* hysteresis effect of polymer materials; charge trapping, ion motion and formation—dissociation of bipolarons in the accumulation layer.[44] In addition, the direct relationship between hysteresis and temperature could be explained with number of the ions. The slope of the each curve also increases with enhancing temperature for P3 thin film.

The temperature dependence of the conductivity in P3 thin film may indicate the conduction mechanism. To provide more detailed information on the conduction mechanism of P3 thin film, dc conductivity value was calculated from the measured current–voltage characteristics by using the following relation[45]:

$$\sigma = \frac{J}{E} = \frac{I.A}{(V/d)} = \frac{I}{V}\frac{d}{(2n-1).l.h} \quad (2)$$

here J is current density, E is electric field, I is the measured current, A is cross-sectional area between the electrodes, h is thickness of the electrodes, V is applied potential, n is the number of fingers of electrodes, and l is overlapping length of fingers. The calculated conductivities are shown in Figure 9 as a function of the operating temperature for P3 thin film at 1 V. The conductivity of the P3 thin film is also given in Figure 9 as a function of reciprocal temperature. Arrhenius plot of lnσ versus 1000/T was used to calculate activation energy (E_A) of the P3 thin film. The results showed that the conductivity of P3 thin film depends exponentially on temperature, which is given in eq. (3):

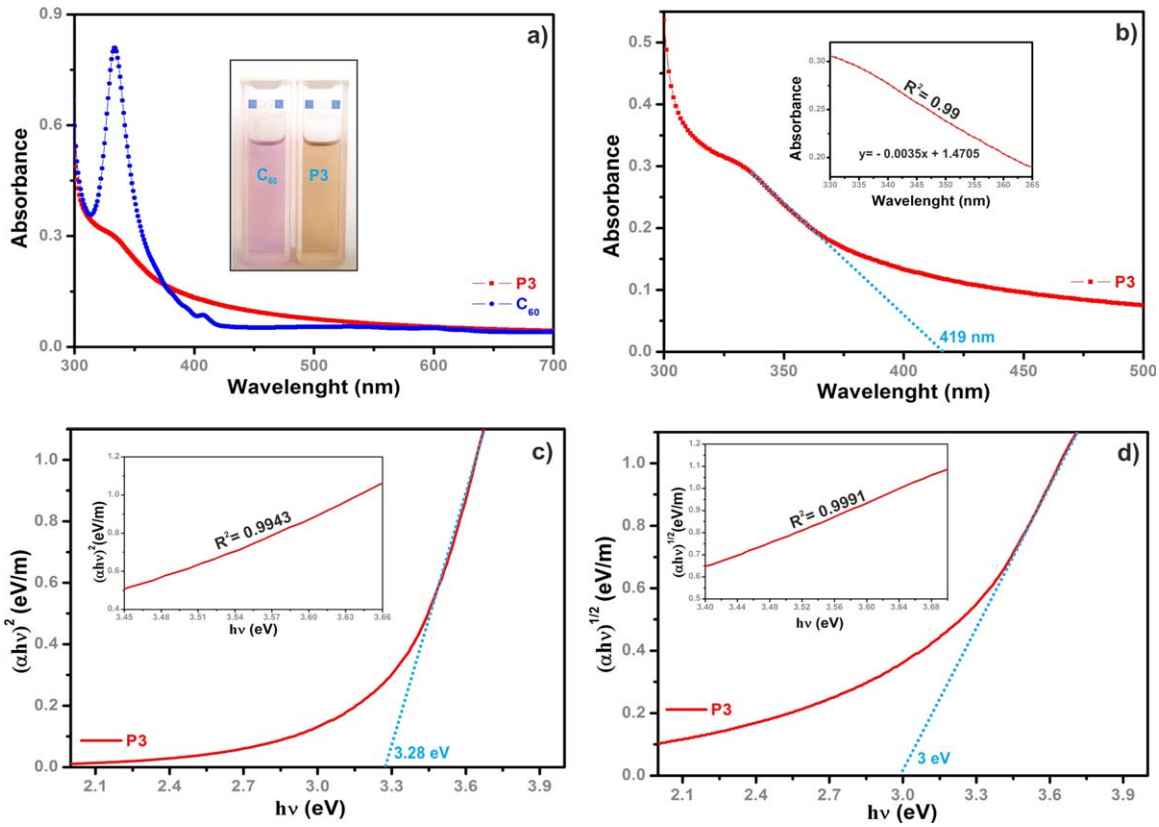

Figure 7. (a) UV–vis spectra of C_{60} and P3 (1×10^{-5} mol/L) in DCB, (b) P3 for measuring λc, (c) plot of $(\alpha h\nu)^2$ versus $h\nu$, and (d) plot of $(\alpha h\nu)^{1/2}$ versus $h\nu$. [Color figure can be viewed in the online issue, which is available at wileyonlinelibrary.com.]

$$\sigma = \sigma_0 \; exp \left({}^{-E_A}/_{kT} \right) \tag{3}$$

where E_A is activation energy, T is temperature, k is Boltzmann's constant and σ_0 is a constant of proportionality. Temperature dependent electrical characterization results show that P(S-*co*-CMS-C_{60}) thin film behaves as a semiconductor in the measured temperature range (303–373 K). It is obvious that at higher temperatures the DC conductivity increased rapidly as seen in Figure 9. This is due to the fact that at higher temperatures, movement of polymer chain segments is thermally enhanced.[46] It would increase assisting and resulting in the increase in conductivity. The activation energy of the sample was evaluated from the slope of the $\ln(\sigma_{dc})$ versus $1/T$ graph and was found between 0.68 eV. The well-defined straight line obtained from the Arrhenius plot suggests the presence of only one conduction mechanism in the temperature range of 303–373 K for the P3 thin film. In systems that obey the Arrhenius dependence the "thermal activated" carriers have sufficent energy to overcome the E_A energy barrier, i.e., thus this behavior is mainly observed at high temperature.[47]

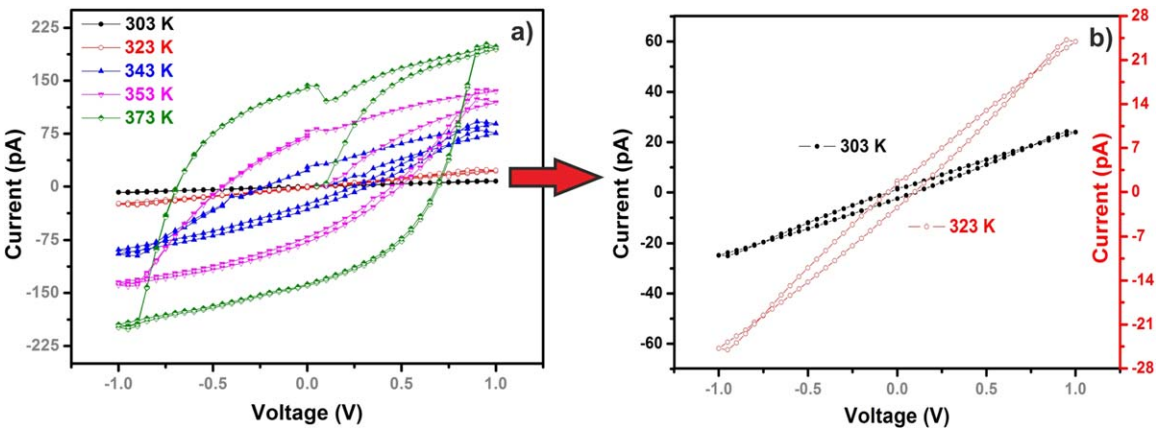

Figure 8. Electrical measurement of P3 at (a) all scale, (b) scale of low temperatures. [Color figure can be viewed in the online issue, which is available at wileyonlinelibrary.com.]

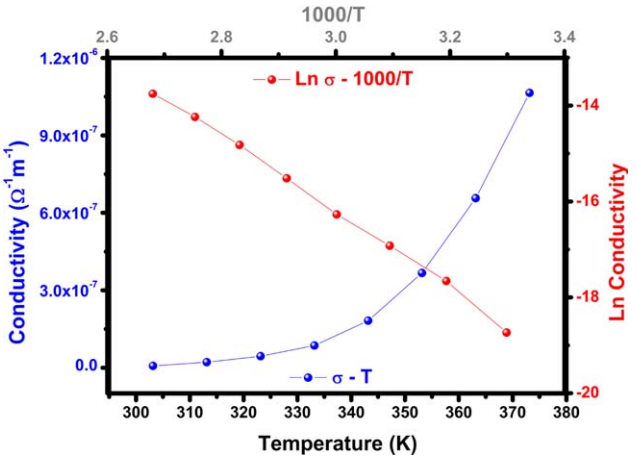

Figure 9. Temperature dependence of the dc conductivity. [Color figure can be viewed in the online issue, which is available at wileyonlinelibrary.com.]

Several studies in the literature about the electrical properties are given as follow. Basavaraja *et al.*, studied the temperature dependent conductivity of the polypyrrole (PPy)–alginate (Ag) blend films.[48] They calculated three values of E_A from the slope of $\log\sigma - 1000/T$ for synthesized polymer blends and found the type of typical electronic conduction in between 0.456 and 0.712 eV for polymer blends while the values in excess of 0.8 eV are attributed to ionic conduction.[48] Aziz *et al.*[46] investigated to the electrical properties of solid polymer electrolyte based on chitosan:$NaCF_3SO_3$. They notified that CS10 sample indicate the Arrhenius behavior of CS:NaTf SPEs and the increase of DC conductivity with increasing temperature is due to the increase of carrier density.[46] G. Sberveglieri and coworkers reported[31] that the current rise of C_{60} thin film (180 nm) deposited on alumina can be fitted by the exponential function $I = I_0\ e^{-E_A/kT}$ with an activation energy E_A equal to 0.7 eV. Harun *et al.*, investigated the electrical conductivity of the blend of polypyrrole doped with iron (III) chloride in PVA matrix at different temperatures. They reported that the dc conductivity increases with the increase of the temperature and indicates that it is fitted to the Arrhenius exponential law equation.[49]

Gas Sensing Properties

P3 thin film devices were used to test H_2, TEA, acetone, and ethanol sensing properties at 100 °C as seen in Figure 10. The sensor had only clear response to H_2 gas at 100 °C. The sensor was not sensitive against acetone and ethanol gases of 5000 ppm. The sensor did not also respond against TEA and H_2 at 30 and 50 °C. For gas sensor measurements, 5000 ppm TEA and 250–2000 ppm H_2 were sent into the measurement cell and after several minutes waiting time, the chamber was cleaned with approximately 200 sccm high purity dry air flow for 15 min. As such, a higher operating temperature leads to a greater change in conductance and hence, greater response. However, the maximum temperature was chosen as the temperature of 100 °C to avoid the decomposition of P3. It is well known that mostly carbon atom is accessible to the gas because they are the surface atoms and gas sensing for P3 may depend on the surface interaction between the gas and π electrons in C_{60}s. While the copolymer chain provides solubility, C_{60} moieties ensure the sensing.[50] The current values of P3 thin film increase and reach the saturation in 10 min when exposed to 5000 ppm TEA at 100 °C as seen in Figure 10(a). During the gas exposure, the current of P3 thin film increases, and then the rate of increment slow down. After the flow of TEA is stopped (cleaning process), the current of P3 thin film recovers to the baseline for 15 min. Similar behavior is observed for H_2 measurement of P3 thin film. The baseline current of P3 thin film changed to 4.01 pA from 5.2 pA in 15 min when the sensor was exposed to 2000 ppm H_2 as seen in the inlet of Figure 10(b). Then, the sensor is purged with dry air for several minutes. While purging the sensor, the current decreases, and then the rate of reduction slows down until it reaches to the baseline. The sensitivity (S) of the sample was evaluated using the response definition:

$$S = \frac{\Delta I}{I_0} = \frac{I_g - I_0}{I_0} \quad (2)$$

where ΔI is the change in current, I_g is the maximum current after the sensor is exposed to the gas, and I_0 is the baseline

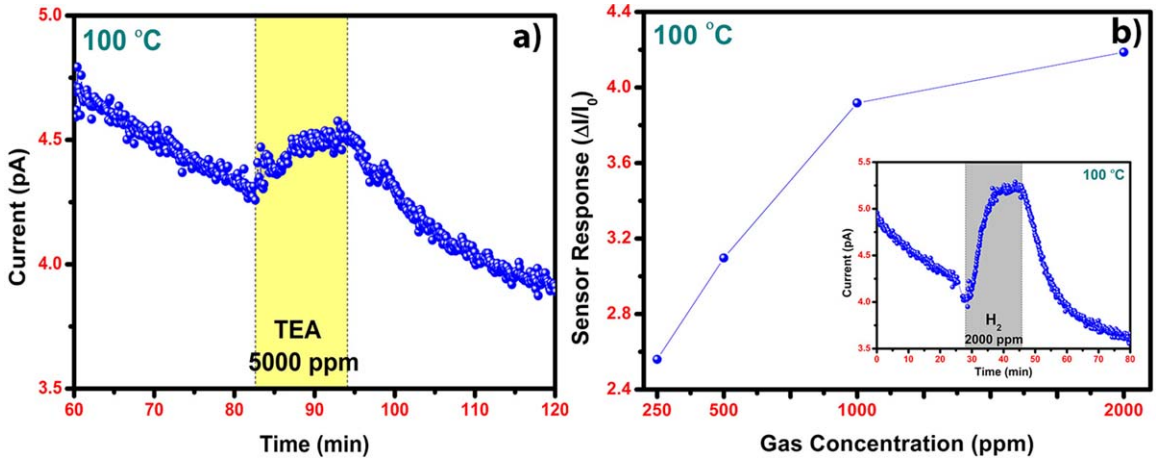

Figure 10. (a) Current–time result of P3 at 100 °C against TEA, (b) H_2 concentration dependent sensitivity result of P3 at 100 °C (inlet: current–time result of P3 against 2000 ppm H_2). [Color figure can be viewed in the online issue, which is available at wileyonlinelibrary.com.]

current (minimum current) of the sensor when exposed to high-purity dry air. The sensitivity of P3 thin film towards to 5000 ppm TEA is evaluated as 0.21. TEA concentration could not determined in this manuscript. Because the sensor was not sensitive for under 5000 ppm of TEA. The upper concentration was so high that the measurement was not needed. In addition, the sensitivity of P3 thin film against 1000 ppm H_2 is calculated as 3.91 at 100 °C as seen in Figure 10(b). TEA sensing properties of the P3 sensor was so low and unclear comparing with H_2 measurement. However, TEA measurement result of the P3 sensor was significant when evaluated singly.

Sberveglieri *et al.* reported C_{60}'s sensing properties towards H_2.[31] They could use thermal evaporation method to coat C_{60} thin film (180 nm) on alumina substrate, which made in harsh condition due to vacuum sublimation of C_{60}. They also obtained 0.2 of sensitivity toward 1000 ppm H_2 in dry air at 300 °C. On the other hand, the sensor used in this study was fabricated via spin coating method with C_{60} containing styrene based soluble copolymer, and also showed a better sensitivity (3.91) against 1000 ppm H_2 in dry air even at 100 °C.

CONCLUSIONS

A a novel styrene copolymer, (P3), having α-thiophene-end group and C_{60} pendant moieties were prepared by nitroxide-mediated radical polymerization (NMP) technique using benzoyl peroxide (BPO) as the radical initiator and nitroxy-functional thiophene compound (Thi-TEMPO) as the co-radical. The attachment of pendant C_{60} groups was achieved with post polymerization reaction. Its detailed characterization was given and the results showed that C_{60} moiety was successfully incorporated into P3 as side group. The presence of C_{60} side-groups has enhanced the thermal stability of P3. UV–vis analysis revealed that P3 has indirect transition. P3 thin film has also a feature of an electronically semiconductor. P3 was then utilized as the sensing material to detect TEA and H_2 at 100 °C. The sensitivity of P3 was found to be much better for H_2. Further studies on the use of P3 in organic/inorganic heterostructures for gas sensing are now in progress.

ACKNOWLEDGMENTS

This work has been partially funded by the Scientific and Technological Research Council of Turkey (TUBITAK), Project Number: 113F403.

REFERENCES

1. Ryntz, R. A.; Yaneff, P. V. Coatings of Polymers and Plastics, 1st ed.; CRC Press: New York, **2003**.
2. Awaja, F.; Gilbert, M.; Kelly, G.; Fox, B.; Pigram, P. *J. Prog. Polym. Sci.* **2009**, *34*, 948.
3. Alavi, S.; Thomas, S.; Sandeep, K. P.; Kalarikkal, N.; Varghese, J.; Yaragalla, S. Polymers for Packaging Applications, 1st ed.; CRC Press: Oakville, **2015**.
4. Sen, A. K. Coated Textiles, Principles and Applications, 2nd ed.; CRC Press: Boca Raton, **2008**.
5. Hollaway, L. Polymer Composites for Civil and Structural Engineering, 1st ed.; Springer: New Delhi, **1993**.
6. Wong, C. P. Polymers for Electronic & Photonic Application, 1st ed.; Academic Press: San Diego, **1993**.
7. Sastri, V. R. Handbook of Polymer Applications in Medicine and Medical Devices, 2nd ed.; William Andrew: Waltham, **2014**.
8. Ebewele, R. O. Polymer Science and Technology, 1st ed.; CRC Press: Boca Raton, **2000**.
9. Matyjaszewski, K.; Sumerlin, B.; Tsarevsky, N. V. Progress in Controlled Radical Polymerization: Materials and Applications, 1st ed.; American Chemical Society: Washington, **2012**.
10. Zhang, H. *Eur. Polym. J.* **2013**, *49*, 579.
11. Wang, C.; Wu, Y.; Tan, S.; Liang, T.; Yang, X. *J. Appl. Polym. Sci.* **2015**, *132*, DOI: 10.1002/app.41564.
12. Leir, C. M.; Galkiewicz, R. K.; Kantner, S. S.; Mazurek, M. *J. Appl. Polym. Sci.* **2010**, *117*, 756.
13. Giacalone, F.; Martin, N. *Chem. Rev.* **2006**, *106*, 5136.
14. Wang, C.; Guob, Z.-X.; Fua, S.; Wub, W.; Zhub, D. *Prog. Polym. Sci.* **2004**, *29*, 1079.
15. Politakos, N.; Grana, E.; Zalakain, I.; Katsigiannopoulos, D.; Eceiza, A.; Kortaberria, G.; Avgeropoulos, A. *J. Appl. Polym. Sci.* **2013**, *131*, DOI: 10.1002/app.40084.
16. Lin, H.-B.; Shih, J.-S. *Sensors Actuat. B Chem.* **2003**, *92*, 243.
17. He, Y.; Hou, J.; Tan, Z.; Li, Y. *J. Appl. Polym. Sci.* **2009**, *115*, 532.
18. Politakos, N.; Zalakain, I.; Fernandez d'Arlas, B.; Eceiza, A.; Kortaberria, G. *Mater. Chem. Phys.* **2013**, *142*, 387.
19. Wang, X.; Goh, S. H.; Lu, Z. H.; Lee, S. Y.; Wu, C. *Macromolecules* **1999**, *32*, 2786.
20. Jiang, G.; Zheng, Q.; Yang, D. *J. Appl. Polym. Sci.* **2005**, *99*, 2874.
21. Taton, D.; Angot, S.; Gnanou, Y. *Macromolecules* **2005**, *38*, 9889.
22. Nava, M. G.; Setayesh, S.; Rameau, A.; Masson, P.; Nierengarten, J. *New J. Chem.* **2002**, *26*, 1584.
23. Lee, T.; Park, O.; Kim, J.; Kim, Y. C. *Chem. Mater.* **2002**, *14*, 4281.
24. Kost, A.; Dougherty, T. K.; Elias, W. E.; Tutt, L.; Klein, M. B. *Opt. Lett.* **1993**, *18*, 334.
25. Dennler, G.; Scharber, M. C.; Brabec, C. J. *Adv. Mater.* **2009**, *21*, 1323.
26. Hwa Hong, K.; Wha Oh, K.; Jin Kang, T. *J. Appl. Polym. Sci.* **2004**, *92*, 37.
27. Lin, C. W.; B. Hwang, J.; Lee, C. R. *J. Appl. Polym. Sci.* **1999**, *73*, 2079.
28. Wunsch, J. R. Polystyrene: Synthesis, Production and Applications, 1st ed.; Rapra Technology Ltd.: Shrewsbury, **1999**.
29. Lia, J. R.; Xub, J. R.; Zhangb, M. Q.; Ronga, M. Z. *Carbon* **2003**, *41*, 2353.
30. Zhang, B.; Fu, R. W.; Zhang, M. Q.; Dong, X. M.; Lan, P. L.; Qiu, J. S. *Sensors Actuat. B: Chem.* **2005**, *109*, 323.
31. Sberveglieri, G.; Faglia, G.; Perego, C.; Nelli, P.; Marks, R. N.; Virgili, T.; Taliani, C.; Zamboni, R. *Synth. Met.* **1996**, *77*, 273.

32. Aydın, M.; Esat, B.; Kılıç, Ç.; Köse, M. E.; Ata, A.; Yılmaz, F. *Eur. Polym. J.* **2011**, *47*, 2283.
33. Karagollu, O.; Gorur, M.; Gode, F.; Sennik, B.; Yilmaz, F. *Sens. Actuators B: Chem.* **2014**, *193*, 788.
34. Dai, S.; Ravi, P.; Tan, C. H.; Tam, K. C. *Langmuir* **2004**, *20*, 8569.
35. Zhang, W.-B.; Tu, Y.; Ranjan, R.; VanHorn, R. M.; Leng, S.; Wang, J.; Polce, M. J.; Wesdemiotis, C.; Quirk, R. P.; Newkome, G. R.; Cheng, S. Z. D. *Macromolecules* **2008**, *41*, 515.
36. Sun, Y.-P.; Riggs, J. E. *J. Chem. Soc. Faraday Trans.* **1997**, *93*, 1965.
37. Zheng, J.; Goh, S. H.; Lee, S. Y. *Polym. Bull.* **1997**, *39*, 79.
38. Katiyar, R.; Bag, D. S.; Nigama, I. *Thermochim. Acta* **2013**, *557*, 55.
39. Yu, H.; Gan, L. H.; Hu, X.; Gan, Y. Y. *Polymer* **2007**, *48*, 2312.
40. Piotrowski, P.; Pawłowska, J.; Pawłowski, J.; Czerwonka, A. M.; Bilewicza, R.; Kaim, A. *RSC Adv.* **2015**, *5*, 86771.
41. Martinez, G.; Gomez, M.; Gomez, R.; Segura, *J. Polym. Sci. Pol. Chem.* **2007**, *45*, 5408.
42. Damlin, P.; Hätönen, M.; Domínguez, S. E.; Ääritalo, T.; Kiveläa, H.; Kvarnströma, C. *RSC Adv.* **2014**, *4*, 8391.
43. Kai, W.; Hua, L.; Dong, T.; Pan, P.; Zhu, B.; Inoue, Y. *Macromol. Chem. Phys.* **2008**, *209*, 104.
44. Paasch, G.; Scheinert, S.; Herasimovich, A.; Hörselmann, I.; Lindner, T. *Phys. Status Solidi A* **2008**, *205*, 534.
45. Şenniķ, E.; Kerli, S.; Alver, Ü.; Öztürk, Z. Z. *Sens. Actuators B: Chem.* **2015**, *216*, 49.
46. Aziz, S. B.; Abidin, Z. H. Z. *J. Soft Matter* **2013**, *2013*, 323868.
47. Utracki, L. A. In High Temperature Polymer; Demeuse, M. T., Eds.; Woodhead Publishing: Cambridge, **2014**; Chapter 3, pp 70–129.
48. Basavaraja, C.; Jo, E. A.; Kim, B. S.; Kim, D. G.; Huh, D. S. *Macromol. Res.* **2010**, *18*, 1037.
49. Harun, M. H.; Saion, E.; Kassim, A.; Hussain, M. Y.; Mustafa, I. S.; Omer, M. A. A. *Malaysian Polym. J.* **2008**, *3*, 24.
50. Sharma, S.; Hussain, S.; Singh, S.; Islam, S. S. *Sens. Actuators B: Chem.* **2014**, *194*, 213.